ROLE OF IRF-8 IN THE INTERFACE OF MELANOMA TUMOR CELL-IMMUNE SYSTEM INTERACTION.

Fabrizio Mattei, Giovanna Schiavoni, Massimo Spada, Francesca Spadaro and Lucia Gabriele

Department of Cell Biology and Neurosciences, Istituto Superiore di Sanità, Rome, Italy.

ABSTRACT

Interferon regulatory factor 8 (IRF-8), is essential for differentiation and function of defined dendritic cell (DC) populations and thus for the induction of competent immune responses. Moreover, IRF-8 acts as a tumor suppressor gene in different types of malignancies.

Recent evidence suggest that DCs are critical players in the immunosurveillance against tumors and that tumor-infiltrating DC (TIDC) may affect the development of antitumor responses. However, the mechanisms underlying DC/tumor cell interaction and the contribution of different DC subtypes at the tumor site remain unclear.

Here, we investigated the role of IRF-8 in affecting immune response against melanoma. To this end, we transplanted B16-F10 metastatic melanoma cells into immunocompetent (WT) and IRF-8-deficient (IRF-8 KO) mice. We found that melanoma expanded rapidly in IRF-8 KO mice whereas its growth was more restrained in WT animals. In fact, IRF-8 KO mice exhibited remarkably higher tumor growth, in terms of mean volume and diameter, which resulted in reduced survival rates with respect to WT counterparts.

We examined the immune cells infiltrating melanomas in WT and IRF-8 KO mice and found severe reduction of TIDC in IRF KO mice, including those subsets that are present in normal number in these mice, namely CD8α$^-$CD11b$^+$ DCs, with respect to WT mice, which exhibited substantial infiltration of this DC subset.

To test whether the expression of IRF-8 itself in melanoma cells could be modulated during tumor growth, we examined the levels of IRF-8 mRNA in melanoma cells excised from tumor-bearing WT and IRF-8 KO mice at different times, when the tumor size was approximately small, medium and large. Surprisingly, IRF-8 was highly expressed in melanomas grown in WT hosts at each tumor stage analysed, whereas it was undetectable in all tumors developed in IRF-8 KO mice.

These results reveal a critical role of IRF-8 in controlling melanoma growth and suggest that IRF-8-mediated antitumor activity is the result of a coordinated action between DC-mediated immune response and the tumor suppressor function of IRF-8. Our data suggest that these two functions may be tightly connected and open new perspectives in understanding the complex mechanisms of tumor cell/immune system interaction.

The transcription factor IRF-8: roles in immunity and tumors

Roles in Immune system

- Transcription factor belonging the Interferon Regolatory Factors (IRFs) family
- Regulator of immune responses against pathogens
- Growth of hematopoietic cells
- Development and maturation of mouse plasmacytoid DCs, CD8α$^+$ DCs and skin DCs
- IRF-8 Knock-out mice: reduced immune responses towards various pathogens

Roles in tumor development: IRF-8 as a tumor suppressor gene

- IRF-8 deficiency speeds up the development of leukemias
- Induction of lung metastasis by repression of IRF-8 after transplantation of a sarcoma CMS4 tumor cell line
- Sarcoma cell line silenced with an IRF-8 siRNA and transplanted in WT immunocompetent mice displayed increased tumor expansion compared to mice transplanted with the same cells not silenced

Melanoma tumors develop faster in IRF-8$^{-/-}$ mice than in normal animals

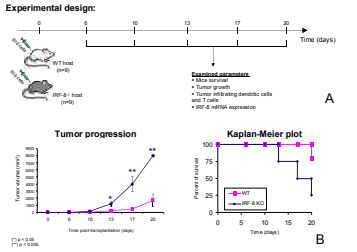

Figure 1. Analysis of melanoma tumor progression in IRF-8$^{-/-}$ mice.

(A) WT and IRF-8$^{-/-}$ mice were injected intracutaneously with 0.8x10^6 B16-F10 melanoma cells and the illustrated parameters were examined at the given timepoints. **(B)** *Left panel*: Growth of melanoma tumors were detected at the given timepoints post-injection. Data show mean tumor volume ± SD. Tumor volumes were calculated by the formula $V=(d_{min} \times d_{max}^2)/2$, where d_{max} and d_{min} are respectively the major and minor diameters of the tumor. *Right panel*: Within the same experiment, the surviving WT and IRF-8-/- mice were counted at each indicated timepoint and the percentage of survival of WT and IRF-8$^{-/-}$ mice was calculated. Levels of significance for comparison between samples were determined by the two-tailed Student's *t* test.

IRF-8$^{-/-}$ mice displayed a defective tumor infiltration of DCs and T cells

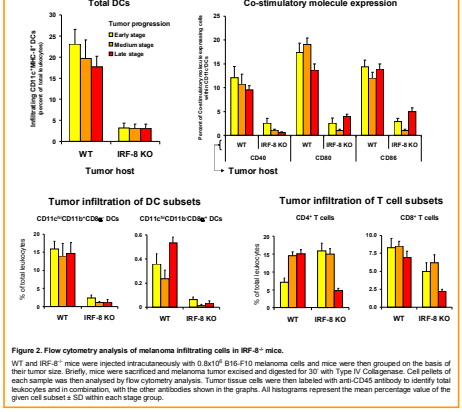

Figure 2. Flow cytometry analysis of melanoma infiltrating cells in IRF-8$^{-/-}$ mice.

WT and IRF-8$^{-/-}$ mice were injected intracutaneously with 0.8x10^6 B16-F10 melanoma cells and mice were then grouped on the basis of their tumor size. Briefly, mice were sacrificed and melanoma tumor excised and digested for 30' with Type IV Collagenase. Cell pellets of each sample was then analysed by flow cytometry analysis. Tumor tissue cells were then labeled with anti-CD45 antibody to identify total leukocytes and in combination, with the other antibodies shown in the graphs. All histograms represent the mean percentage value of the given cell subset ± SD within each stage group.

IRF-8 mRNA expression is downregulated in B16 melanomas grown in IRF-8$^{-/-}$ hosts

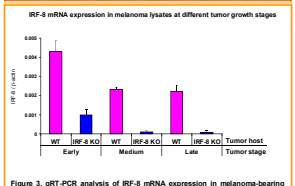

Figure 3. qRT-PCR analysis of IRF-8 mRNA expression in melanoma-bearing IRF8$^{-/-}$ mice.

WT and IRF-8$^{-/-}$ mice were injected intracutaneously with 0.8x10^6 B16-F10 melanoma cells and mice were then grouped on the basis of their tumor size. Melanoma tumors were excised from each mouse and digested for 30' with Type IV Collagenase. Real-time qRT-PCR was then performed on melanoma lysates by using IRF-8-specific and β-actin-specific primers. For quantitation, threshold cycle (C_T) values were determined by the Sequence Detection System software (Applied Biosystems), and ΔC_T was obtained by subtracting C_T of reference mRNA, β-actin, to C_T of IRF-8 mRNA. The amount of mRNA, normalised to β-actin, was calculated as $2^{-\Delta CT}$.

5-Aza-dC-driven hypomethylation leads to increased levels of IRF-8 in B16 melanoma cells *in vitro*

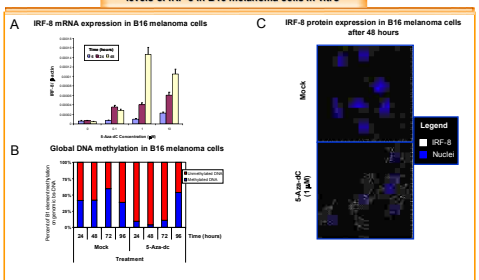

Figure 4. Analysis of IRF-8 expression in B16 melanoma tumor cells following treatment with 5-Aza-dC.

(A) B16-F10 melanoma cells (0.3x10^6 cells) were cultured for the indicated times using the different 5-Aza-2'-deoxycytidine (5-Aza-dC) concentrations displayed in the graph. Total RNA from each experimental condition was purified. qRT-PCR was then performed by using IRF-8-specific and β-actin-specific primers as described in *Figure 3*. **(B)** B16-F10 tumor cells were cultured with or without 5-Aza-dC at the concentration of 1μM. At the indicated culture times, tumor cells were resuspended with a Trypsin buffer and genomic DNA from each sample was purified. DNA was then bisulfite-converted and a qPCR was performed onto the obtained genomic bisulfite DNA by using two primer pairs detecting methylation or demethylation of the B1 element. Histograms represent the percentage of DNA methylation detected within the B1 element. **(C)** B16-F10 melanoma cells were cultured for 48 hours with or without 5-Aza-dC (1 μM) and then fixed *in situ* with methanol. A primary anti-IRF-8 antibody is used to determine expression of IRF-8 into cytoplasm and nuclei by confocal microscopy analysis.

5-Aza-dC decreases the proliferation, invasiveness and migration ability of B16 melanoma cells

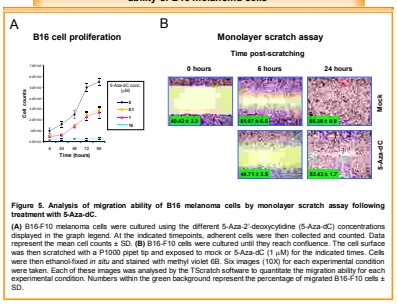

Figure 5. Analysis of migration ability of B16 melanoma cells by monolayer scratch assay following treatment with 5-Aza-dC..

(A) B16-F10 melanoma cells were cultured using the different 5-Aza-2'-deoxycytidine (5-Aza-dC) concentrations displayed in the graph legend. At the indicated timepoints, adherent cells were then collected and counted. Data represent the mean cell counts ± SD. **(B)** B16-F10 cells were cultured until they reach confluence. The cell surface was then scratched with a P1000 pipet tip and exposed to mock or 5-Aza-dC (1 μM) for the indicated times. Cells were then ethanol-fixed *in situ* and stained with methyl violet 6B. Six images (10X) for each experimental condition were taken. Each of these images was analysed by the TScratch software to quantitate the migration ability for each experimental condition. Numbers within the green background represent the percentage of migrated B16-F10 cells ± SD.

Injection of 5-Aza-dC in IRF-8$^{-/-}$ hosts induces a transient melanoma regression

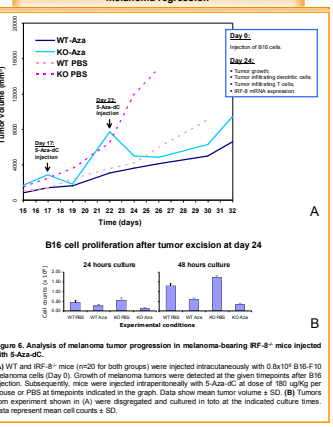

Figure 6. Analysis of melanoma tumor progression in melanoma-bearing IRF-8$^{-/-}$ mice injected with 5-Aza-dC.

(A) WT and IRF-8$^{-/-}$ mice (n=20 for both groups) were injected intracutaneously with 0.8x10^6 B16-F10 melanoma cells (Day 0). Growth of melanoma tumors were detected at the given timepoints after B16 injection. Subsequently, mice were injected intraperitoneally with 5-Aza-dC at dose of 180 ng/Kg per mouse or PBS at timepoints indicated in the graph. Data show mean tumor volume ± SD. **(B)** Tumors from experiment shown in (A) were disgregated and cultured in toto at the indicated culture times. Data represent mean cell counts ± SD.

Injection of 5-Aza-dC in IRF-8$^{-/-}$ hosts leads to IRF-8 promoter demethylation and restores the expression of IRF-8 mRNA within their tumor lysates

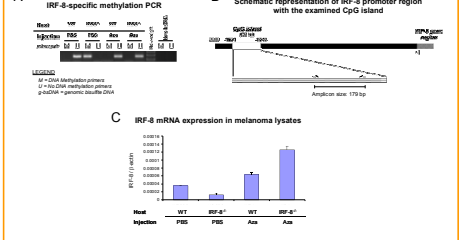

Figure 7. Analysis of IRF-8 promoter methylation and IRF-8 mRNA expression in melanoma-bearing IRF-8-/- mice following injection of 5-Aza-dC.

WT and IRF-8$^{-/-}$ mice were injected with B16 melanoma cells and 5-Aza-dC as specified in the experiment shown in *Figure 6*. Animals were sacrificed and melanoma tumor tissue were excised and then pooled into the four experimental conditions specified in *(A)* and *(C)*. **(A)** Methylation of the IRF-8 promoter was analysed by methylation-specific PCR onto a CpG island within the IRF-8 promoter illustrated in *(B)*. Genomic, bisulfite-converted DNA samples derived from experiment shown in Figure 6 was used. **(C)** qRT-PCR performed with IRF-8-specific primers to determine the expression levels of IRF-8 mRNA within the four groups. Arrows in *(B)* represent the primer pairs used in this methylation-specific PCR assay. Pink lines indicate the CpG spots detected by MethylPrimer Express software.

Injection of 5-Aza-dC in IRF-8$^{-/-}$ hosts leads to increased expression levels of Type I Interferons within the relative melanoma lysates

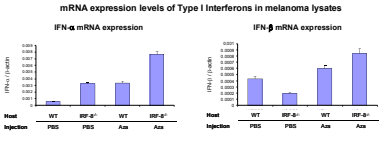

Figure 8. Detection of expression levels of Type I Inteferons by qRT-PCR in melanoma-bearing IRF-8-/- mice treated with 5-Aza-dC.

WT and IRF-8$^{-/-}$ mice were injected with B16 tumor cells and 5-Aza-dC as specified in *Figure 6*. Mice were sacrificed and melanoma tumor tissue were excised and then pooled into the four experimental conditions specified below the histograms. Tumor tissues groups were digested for 30' with Type IV Collagenase and total RNA from each melanoma lysate was purified. Quantitative (real-time) RT-PCR was then performed with IFN-α-specific and IFN-β-specific primers (*Left panel* and *Right panel*, respectively).

Injection of 5-Aza-dC in IRF-8$^{-/-}$ hosts leads to increased expression levels of Type I Interferons within the relative melanoma lysates

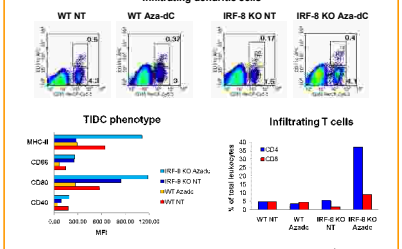

Figure 9. Flow cytometry analysis of melanoma infiltrating cells in melanoma-bearing IRF-8$^{-/-}$ mice following treatment with 5-Aza-dC.

WT and IRF-8$^{-/-}$ mice were injected with B16 tumor cells and 5-Aza-dC as specified in *Figure 6*. Mice were sacrificed and melanoma tumor tissue were excised and then pooled into the four experimental conditions indicated in all the graphs. The pooled samples were then analysed by flow cytometry analysis. Tumor tissue cells were then labeled with anti-CD45 antibody to identify total leukocytes and in combination, with the other antibodies shown in the graphs. All histograms represent the mean percentage value of the given cell subset ± SD within each experimental condition.

References

Holtschke, T., J. Lohler, Y. Kanno, T. Fehr, N. Giese, F. Rosenbauer, J. Lou, K.P. Knobeloch, L. Gabriele, J.F. Waring, M.F. Bachmann, R.M. Zinkernagel, H.C. Morse, 3rd, K. Ozato, and I. Horak. 1996. Immunodeficiency and chronic myelogenous leukemia-like syndrome in mice with a targeted mutation of the ICSBP gene. *Cell* 87:307-317.

Schiavoni, G., F. Mattei, P. Sestili, P. Borghi, M. Venditti, H.C. Morse, 3rd, F. Belardelli, and L. Gabriele. 2002. ICSBP is essential for the development of mouse type I interferon-producing cells and for the generation and activation of CD8alpha(+) dendritic cells. *J Exp Med* 196:1415-1425.

Schiavoni, G., F. Mattei, P. Borghi, P. Sestili, M. Venditti, H.C. Morse, 3rd, F. Belardelli, and L. Gabriele. 2004. ICSBP is critically involved in the normal development and trafficking of Langerhans cells and dermal dendritic cells. *Blood* 103:2221-2228.

Mattei, F., G. Schiavoni, P. Borghi, M. Venditti, I. Carini, P. Sestili, I. Pietraforte, H.C. Morse, 3rd, C. Ramoni, F. Belardelli, and L. Gabriele. 2006. ICSBP/IRF-8 differentially regulates antigen uptake during dendritic-cell development and affects antigen presentation to CD4+ T cells. *Blood* 108:809-817.

Yang, D., M. Thangaraju, K. Greenlich, D.D. Browning, P.V. Schoenlein, T. Tamura, K. Ozato, V. Ganapathy, S.I. Abrams, and K. Liu. 2007. Repression of IFN regulatory factor 8 by DNA methylation is a molecular determinant of apoptotic resistance and metastatic phenotype in metastatic tumor cells. *Cancer Res* 67:3301-3309.

Koeningsmann, J., C. Rudolph, S. Sander, O. Kershaw, A.D. Gruber, L. Bullinger, B. Schlegelberger, and D. Carstanjen. 2009. NF1 haploinsufficiency and lostp deficiency synergize in the development of leukemias. *Blood* 113:4690-4701.

Kantarjian, H., J.P. Issa, C.S. Rosenfeld, J.M. Bennett, M. Albitar, J. DiPersio, V. Klimek, J. Slack, C. de Castro, F. Ravandi, R. Helmer, 3rd, L. Shen, S.D. Nimer, R. Leavitt, A. Raza, and H. Saba. 2006. Decitabine improves patient outcomes in myelodysplastic syndromes: results of a phase III randomized study. *Cancer* 106:1794-1803.

Issa, J.P., and H.M. Kantarjian. 2009. Targeting DNA methylation. *Clin Cancer Res* 15:3938-3946.

Garcia-Manero, G. 2008. Demethylating agents in myeloid malignancies. *Curr Opin Oncol* 20:705-710.

Liang, C.C., A.Y. Park, and J.L. Guan. 2007. *In vitro* scratch assay: a convenient and inexpensive method for analysis of cell migration in vitro. *Nat Protoc* 2:329-333.

Greenlich, K.M., M. Schneider, S.M. Steinberg, D.J. Liewehr, T.J. Stewart, K. Liu, and S.I. Abrams. 2007. Host immunosurveillance controls tumor growth via IFN regulatory factor-8 dependent mechanisms. *Cancer Res* 67:10406-10416.

SUMMARY AND CONCLUSIONS

Mice lacking IRF-8 expression display faster growth of transplanted B16 melanoma, which associates with reduced tumor infiltration by DC, CD8$^+$ and CD4$^+$ T lymphocytes and with down-regulation of IRF-8 expression in B16 tumors.

Restoration of IRF-8 expression by 5-Aza-dC treatment leads to a transient arrest of melanoma growth in IRF-8$^{-/-}$, but not in control mice.

The selective action of 5-Aza-dC in IRF-8$^{-/-}$ hosts is associated to:

- IRF-8 switching in transplanted B16 melanomas
- Enhanced tumor infiltration by functionally activated DC and by T cells
- High intratumoral expression levels of Type I Interferons

Intratumoral expression of IRF-8 generates a dual effect in the context of melanoma development:

- It allows IRF-8 to function as a tumor suppressor gene, thus leading to melanoma tumor regression
- It promotes tumor infiltration by T cells and DC which, in turn, may lead to melanoma growth control.

IRF-8 may represent a key factor regulating the interplay between melanoma tumor progression and host immune system